

Model of Visually Evoked Cortical Potentials

J. KREMLÁČEK, M. KUBA, J. HOLČÍK¹

Department of Pathological Physiology, Medical Faculty of Charles University in Hradec Králové,
¹Department of Biomedical Engineering, Faculty of Electrical Engineering and Computer Science,
Brno University of Technology, Czech Republic

Received January 18, 2001

Accepted June 6, 2001

Summary

The pattern-reversal (P-VEPs) and the motion-onset (M-VEPs) of visual evoked potentials were modeled by means of three damped oscillators (O_1 , O_2 , O_3) of identical construction. The O_1 , assumed to simulate the response of primary visual area (V1), was driven by the firing density of the lateral geniculate nuclei. O_1 contributed mainly to the N_{75} and P_{100} peaks of the P-VEPs. The O_2 , driven by the O_1 output, mimics the activity of V2, V3a, and MT. It contributed to the negative peak N_{145} of the P-VEPs or to the N_{160} in the M-VEPs. The O_3 was suggested to model late slow processes probably of an attentive origin. The model parameters were set by optimization to follow the P-VEPs and M-VEPs obtained as a grand average of four young volunteers ($P_Z - A_2$ lead). The evoked potentials were described with normalized root mean square error lower than 13 %.

Key words

Mathematical model • Visual evoked potentials • Pattern-reversal • Motion-onset

Introduction

Visual evoked potentials (VEPs - brain cortical electric activity related to visual stimuli) represent an objective non-invasive method for theoretical research of visual information processing, as well as a diagnostic tool for early detection of some functional brain disorders - e.g. multiple sclerosis, encephalopathy, dyslexia (Regan 1989, Kubová and Kuba 1992, Nuwer 1998). VEPs enable also an objective testing of visual parameters (such as visual acuity) in poorly co-operating subjects (children, malingers etc.) (Steele *et al.* 1989).

In comparison to the modern brain imaging techniques (i.e. functional magnetic resonance), the VEPs examination is a low price method with very high temporal resolution. The activity corresponding to the

VEPs generation is mediated along the visual pathway from the lateral geniculate nuclei (subcortical visual brain centre) *via* the primary visual cortical area (occipital striate area - V1) to extrastriate associate visual areas specialized for the visual perception (for review see Tootell *et al.* 1998).

Both recognized parallel subsystems of the visual pathway - the parvocellular and magnocellular ones (Livingstone and Hubel 1988) can be tested with the use of various patterns and moving visual stimuli. Compared to the parvocellular system activated mainly by a fine pattern, the magnocellular system has a higher sensitivity at low spatial and high temporal frequencies of visual moving stimuli at low luminance contrast (Derrington and Lennie 1984, Sclar *et al.* 1990).

Standard pattern-reversal VEPs (P-VEPs) and newly introduced motion-onset VEPs (M-VEPs) were simulated in this study, since they are of different origins and display various properties (Kubová *et al.* 1995).

The proposed model is based on the hypothetical functions of morphological structures involved in VEPs formation. An integral view of P-VEPs and M-VEPs generation is presented.

There are basically two different approaches to electroencephalographic activity modeling. The first one — based on single unit studies — describes the behavior and functions of single neurons or simple neuronal circuits. However, we need to model an accessory activity projected onto the human scalp - EPs. Because the EPs have a strong relation to the EEG (electroencephalography) (Başar 1980) and the EEG is closely related to neuronal activity, a neurophysiologically based model of observed alpha EEG oscillations (8-12 Hz) (da Silva and Hoek 1974) and its derivative for flash VEPs (Jansen *et al.* 1993) was one of the sources evaluated for the presented model of VEPs.

The second approach is based on a simplified macroscopic description of the EEG-EPs behavior seen as an oscillation with perturbations, changes of amplitude, frequency and phase. Such processes can be modelled by nonlinear oscillator(s) (see Zeeman 1976a, b, Ingber *et al.* 1995). To test this theory, an attempt was made to decompose the transient pattern-onset VEPs using an analytical solution of the Duffing oscillator (Serebro 1995). This solution provided a good description of the VEPs waveform when three oscillators were combined.

The presented model is derived from both approaches, and it includes macroscopic oscillators with neurophysiologically observed forcing. Functional anatomical relations are respected within its structure.

Methods

Data

A group of four healthy subjects (2 women, 2 men) with no history of visual or neurological disorders was examined. Informed consent with the experiment was obtained from each subject before the experiment.

The stimuli were generated with the use of the animation program Animator Pro (USA) and displayed on a 21" computer monitor ViewSonic (USA) with 75 Hz frame frequency and mean luminance of 17 cd/m². The stimulation field was 45x35 deg at a 0.5 m observing distance. To stimulate the parvocellular system, we used

pattern reversal of 96 % Michelson contrast checkerboard with the check size 40 arc min i.e. spatial frequency of 0.75 deg⁻¹.

Two different routes of movement processing in man have been reported and, therefore, we employed two motion stimuli (ffytche *et al.* 1995). To examine the slow geniculo-striate channel, we used high contrast (96 %) checkerboard (0.75 deg⁻¹) moving at 7 deg/s. A low 10 % contrast isolated checks of 40 arc min with a period of 0.375 deg⁻¹ and a velocity of 14 deg/s were used for the fast tectal channel examination. The high adaptability to motion must be respected in motion-VEP recordings (long inter-stimulus intervals are crucial) (Bach and Ullrich 1994). Therefore, stimulus timing was 0.5 s of the moving and 2.5 s of the stationary stimulus. The structure moved in one of four cardinal directions in a pseudorandom order.

The EEG data were recorded from P_Z, with right ear lobe - A₂ reference. The signal was 20 000 times amplified and filtered with a band pass filter 0.1 to 100 Hz. 512 samples of 250 Hz and 12-bit resolution were recorded. The recording part was synchronized with the stimulus *via* a parallel port and the trigger was applied 1000 ms before a stimulus onset. The data were acquired in three sessions and 20 responses were recorded in each.

For every subject, the recorded set of data was averaged to eliminate spontaneous uncorrelated activity. A single subject contribution was equalized in the group and a normalized group grand average for each stimulus condition was computed.

Model design and data analysis

The structure of the presented model is based on an analysis of the M-VEPs and P-VEPs. The model is based on a generally accepted idea that different neuronal populations can be sequentially activated and may jointly contribute to the final EP in the brain.

The number of modeled neuronal populations was determined by means of principal component analysis (PCA) and independent component analysis (ICA) of the grand average data. It was found that for all stimuli and both analyses, three components describe the data optimally (Kremláček *et al.* 1999).

It was considered under a comparison of a normalized root mean square error (NRMSE) $r_{sim}(1)$ of reconstructed data y and recorded VEPs ep to a relative amount of noise r_n (redundant and non predicable information) (2). The level of noise y_{\pm} was estimated by \pm average (3) (Schimmel 1967).

$$r_{sim} = \sqrt{\frac{\sum(ep - y)^2}{\sum ep^2}} \cdot 100 \quad [\%] \quad 1.$$

$$r_n = \sqrt{\frac{\sum(y_{\pm})^2}{\sum ep^2}} \cdot 100 \quad [\%] \quad 2.$$

$$y_{\pm}(t) = \frac{\sum_{i=1}^n (-1)^i e_i(t)}{n} \quad 3.$$

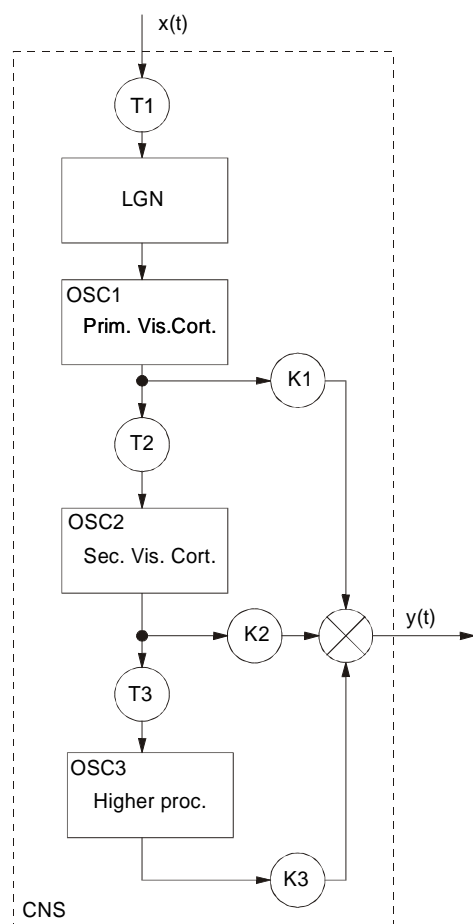


Fig. 1. Block diagram of visual evoked potentials generation. The model is forced with delay T_1 from LGN. Following oscillators represent cortical neural groups activated with a delay T_n and contributing to the final potential according to the weight coefficients K_n . The OSC_1 epitomises the primary visual cortex, the OSC_2 extrastriate areas and a response of OSC_3 mimics probably a higher level of perception.

It was shown that the first component reflects stimulus characteristics (probably activation of the V1), the second one may activate extrastriate areas and is common, together with the third component (rejection of a cognitive processes), among all presented stimuli (Kremláček and Kuba 1999). It can be expected that the three oscillators, similarly to independent components, will exhibit different features of VEPs and therefore a serial connection of oscillators was chosen with delays T_n among them. The contribution of an oscillator, as a cortical source to the scalp potential, is determined in the model by K_n coefficients. The model schema is depicted in the Fig.1. Single neuronal group was modeled as a forced second order nonlinear oscillator (see Fig. 2) This selection was based on the general temporal characteristics of the EP: a slow increase of amplitude followed by a damping of the oscillations while a shift from fast to slow frequencies is continually presented. A simple way to mimic this behavior is to force a simple damped oscillator. The slow increase of amplitudes and the transition to slow frequencies is done by characteristic of a forcing function (this applies for the first oscillator) adopted from the output of the lateral geniculate nuclei (Watson and Nachmias 1977). The oscillator attributes, such as the frequency of relaxed oscillations or the damping magnitude, were set by the a and b coefficients.

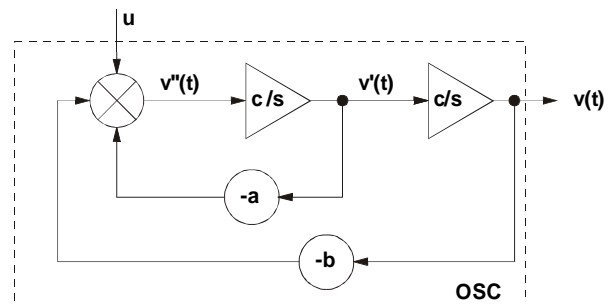


Fig. 2. The schema of the single oscillator as it was modeled in Simulink. The oscillator can be described by the following nonlinear second order equation: $\ddot{v} = u(t) - a\dot{v} - bv$.

The model was simulated in the Matlab-Simulink environment (USA) - see Figure 2. To find the required parameters describing the VEPs, the "downhill-simplex" Nelder-Mead optimization method was utilized (Lagarias *et al.* 1997). The starting - simplex point was determined with the use of a direct search. The simulation underwent the optimization three times and the simplex

point was set as the result of the previous optimization in the second and the third run. The normalized root mean square error function served as the optimization criterion (1).

Results

The recorded data are displayed as the solid thin line in Figs. 3, 4, and 5. The data represent normalized grand average at the parietal recording site P_Z. The major parameters obtained *via* the optimization procedure are listed in Tab. 1 and 2. The simulation results are shown in Figs. 3, 4, and 5. Besides the simulated curves, separate contributions of oscillators are also presented (see the attached legend).

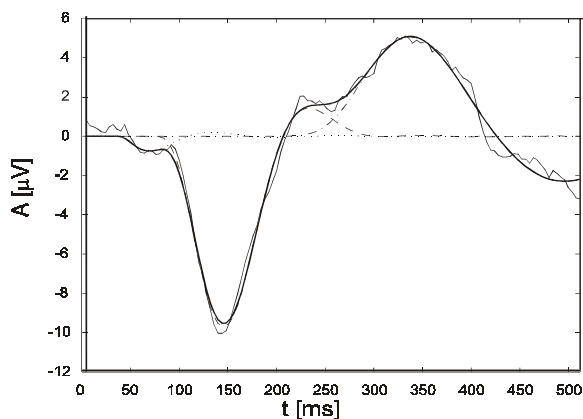


Fig. 3. Recorded (thin solid line) and simulated (bold solid line) motion-onset VEPs to slowly moving (7 deg/s) high contrast (96 %) checkerboard (0.75 deg^{-1}). The contributions of separate oscillators are drawn as dotted (OSC1), broken (OSC2) and broken-dotted (OSC3) line. The NRMSE between recorded and simulated data is 11.85 %.

The accuracy of simulated data fit the original results was expressed by normalized root mean square error r_{sim} in Table 2. The optimization method has shown a strong dependence on the simplex point selection. This sensitivity was overcome by a direct search of this starting point.

There was evidence that the presented values are one of the best solutions, because any other results with a randomly selected simplex produced an inferior fitness after the optimization. It is also documented by the NRMSE, which was lower than 13 % in all cases (see the Table 2).

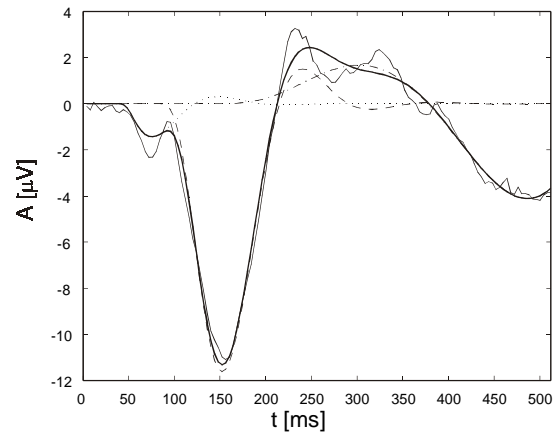


Fig. 4. Recorded and simulated motion-onset VEPs to fast moving (14 deg/s) low contrast (10 %) structure of isolated checks (0.375 deg^{-1}). The figure arrangement is the same as in Fig. 3. The NRMSE between recorded and simulated data is 12.90 %.

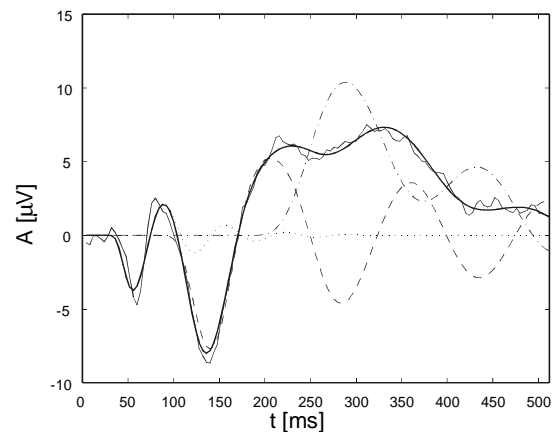


Fig. 5. Recorded and simulated P-VEPs to the pattern-reversal of high contrast (96 %) checkerboard (0.75 deg^{-1}). The figure arrangement is the same as in Fig. 3. The NRMSE between recorded and simulated data is 10.97 %.

Discussion

Two kinds of visual evoked potentials were simulated *via* three serially connected nonlinear oscillators. This approach was based on the data decomposition into independent components (Kremláček and Kuba 1999). A similar approach to simulate another kind of visual evoked potentials, pattern-onset by the Duffing oscillator, was recently employed (Serebro 1995). It is interesting that three oscillators were also selected in this work as the optimum. The agreement between these results in the number of components

Table 1. Contributions (K) and delays (T) of separate oscillators (see Fig. 1)

Stimulus	$K_1[-]$	$K_2[-]$	$K_3[-]$	$T_1[ms]$	$T_2[ms]$	$T_3[ms]$
<i>Slow motion</i>	-0.6912	-1.7850	0.0449	28.8528	34.7407	118.9657
<i>Fast motion</i>	-1.2622	-3.0472	0.0077	33.3449	40.4837	43.5710
<i>Pattern-reversal</i>	-5.2293	-2.4574	0.2404	24.6984	53.1513	6.4955

Table 2. Oscillators frequency of relaxed oscillation. Parameters of correspondence between simulated and recorded data.

Stimulus	$r_{sim}[\%]$	$r_n[\%]$	$f_{osc1} [Hz]$	$f_{osc2} [Hz]$	$f_{osc3} [Hz]$
<i>Slow motion</i>	11.85	13.16	7.8622	3.8337	2.9910
<i>Fast motion</i>	12.90	17.49	6.9276	3.6508	2.6961
<i>Pattern-reversal</i>	10.97	14.66	14.9634	6.6326	1.3386

suggests that the transient visual evoked potentials can be sufficiently described by three damped oscillators. However, their different temporal parameters show that there are either different structures involved in the EPs generation or that the brain generators exhibit different dynamic properties depending on the stimulus parameters. A spatio-temporal model could resolve this question (in preparation).

To assess the simulation fit, we compared NRMSE (r_{sim}) with the signal noise (r_n - see in Table 2). There was good agreement between simulated and recorded data but the three oscillators described the original data with even higher precision than it would have been expected from the noise level (the estimate based on the \pm average). This can be due to the fact that the \pm average is a statistical value and it embodies a convergence fluctuation. The same also holds for EPs, so that we cannot avoid a redundancy in the simulation because there is not exact way of discriminating between the noise and the EPs.

The present model was designed as a connection between neuronal groups imitated by oscillators. One can ask if there is any relation between the obtained results and electrophysiological findings.

It is generally accepted that the P-VEPs are generated in the occipital cortex near the sulcus calcarinus (e.g Arroyo *et al.* 1997). The contributions of the first oscillator to the simulated VEPs suggested that in case of the pattern-reversal VEPs there is much stronger

activation in comparison to the other stimuli. This indicates that the first oscillator is representing the V1 area.

The peak of the second oscillator activity appeared at about 150 ms. A local minimum occurs at this time at the onset of movement and pattern-reversal VEPs, which is connected with extrastriate areas activity, namely MT or MST area (Kubová *et al.* 1995, Bach and Ullrich 1997). The third component peaked at about 300-350 ms, which is typical for late, non-specific attentive or cognitive processing (compare to P300).

When we assume that the second oscillator has some relationship to the MT brain area, it is interesting to note the activation delay. While clinical studies have shown that there is potent activation of this area at about 150 ms (Kuba and Kubová 1992, Bach and Ullrich 1994), very early activation of the MT was reported at about 50 ms (Ffytche *et al.* 1995). In the present model, there is a delay from 63 to 78 ms before the second oscillator activation, but its activity peaks at about 150 ms. This could explain the above mentioned findings.

The proposed serial model design does not seem to be in agreement with the generally accepted parallel organization of the visual pathway. However, the data presented here represent almost exclusively results of relatively selective stimulation of the transient visual separate channels.

Conclusions

The model of visual evoked potentials based on a macroscopic description of neural groups, forced in agreement with electrophysiological findings, is presented as a serial connection of three nonlinear oscillators.

This model successfully simulated pattern-reversal VEPs, motion-onset VEPs of slowly moving objects with high contrast structure, and motion-onset VEPs of a fast moving low contrast structure by a change of oscillator parameters.

Optimized parameters suggest that the oscillators correspond to visual areas or they are associated with

different stages of visual information processing (1. the primary visual area - reception; 2. the secondary visual area - features extraction; 3. higher areas - sensation). The second oscillator in the model mimics the extrastriate activity linked in case of moving stimuli with the mediotemporal area activation. The simulation results have shown that this activity peaked at about 150 ms after starting already 60 - 80 ms after the stimulus onset.

Acknowledgements

Supported by the Czech Ministry of Education (FH MSM 111100008), Grant Agency of the Czech Ministry of Health (Grant No. 4800-3) and by the James S. McDonnell Foundation, USA (99-57EE-GLO.04).

References

- ARROYO S, LESSER R, POON W, WEBBER W, GORDON B: Neuronal generators of visual evoked potentials in humans: visual processing in the human cortex. *Epilepsia* **38**: 600-610, 1997.
- BACH M, ULLRICH D: Motion adaptation governs the shape of motion-evoked cortical potentials. *Vision Res* **34**: 1541-1547, 1994.
- BACH M, AND ULLRICH D: Contrast dependency of motion-onset and pattern-reversal veps: interaction of stimulus type, recording site and response component. *Vision Res* **37**: 1845-1849, 1997.
- BAŞAR E: *EEG-Brain Dynamics, Relation between EEG and Brain Evoked Potentials*. Elsevier, Amsterdam 1980.
- DA SILVA FL, HOEK A: Model of brain rhythmic activity - The alpha-rhythm of the thalamus. *Kybernetik* **15**: 27-37, 1974.
- DERRINGTON A, LENNIE P: Spatial and temporal contrast sensitivities of neurones in lateral geniculate nucleus of macaque. *J Physiol Lond* **375**: 219-240, 1984.
- FFYTCH DH, GUY CN, ZEKI S: The parallel visual motion inputs into areas V1 and V5 of human cerebral cortex. *Brain* **118**: 1375-1394, 1995.
- INGBER L, SRINIVASAN R, NUNEZ P: Path-integral evolution of chaos embedded in noise: Duffing neocortical analog. *Math Comp Model* **23**: 43-53, 1995.
- JANSEN B, ZOURIDAKIS G, BRANDT M: A neurophysiologically-based mathematical model of ash visual evoked potentials. *Biological Cybernetics* **68**: 275-283, 1993.
- KREMLÁČEK J, KUBA M: Global brain dynamics of transient visual evoked potentials. *Physiol Res* **48**: 303-308, 1999.
- KREMLÁČEK J, KUBA M, KUBOVÁ Z, VÍT F: Simple and powerful visual stimulus generator. *Comput Methods Programs Biomed* **58**: 175-180, 1999.
- KUBA M, KUBOVÁ Z: Visual evoked potentials specific for motion-onset. *Doc Ophthalmol* **80**: 83-89, 1992.
- KUBOVÁ Z, KUBA M: Clinical applications of motion-onset VEPs. *Doc Ophthalmol* **81**: 209-218, 1992.
- KUBOVÁ Z, KUBA M, SPEKREIJSE H, BLAKEMORE C: Contrast dependence of motion-onset and pattern-reversal evoked potentials. *Vision Res* **35**: 197-205, 1995.
- LAGARIAS JC, REEDS JA, WRIGHT M, WRIGHT P: Convergence Properties of the Nelder-Mead Simplex Algorithm in Low Dimensions. *SIAM Journal of Optimization*: 112-147, 1997.
- LIVINGSTONE M, HUBEL DH: Segregation of form, color, movement, and depth: anatomy, physiology, and perception. *Science* **240**: 740-749, 1988.
- NUWER M: Fundamentals of evoked potentials and common clinical applications today. *Electroencephalogr Clin Neurophysiol* **106**: 142-148, 1998.

-
- REGAN D: *Human Brain Electrophysiology, Evoked Potentials and Evoked Magnetic Field in Science and Medicine*. Elsevier Science Publishing, New York, 1989.
- SCHIMMEL H: The (\pm) reference: accuracy of estimated mean components in average response studies. *Science* **157**: 92-93, 1967.
- SCLAR G, MAUNSELL J, LENNIE P: Coding of image contrast in central visual pathways of the macaque monkey. *Vision Res* **30**: 1-10, 1990.
- SEREBRO R: The Duffing oscillator: a model for the dynamics of the neuronal groups comprising the transient evoked potential. *Electroencephalogr Clin Neurophysiol* **96**: 561-573, 1995.
- STEELE M, SEIPLE W, CARR R, KLUG R: The clinical utility of visual-evoked potential acuity testing. *Am J Ophthalmol* **108**: 572-577, 1989.
- TOOTELL R, HADJIKHANI N, MENDOLA J, MARRETT S, DALE A: From retinotopy to recognition: fMRI in human visual cortex. *Trends Cogn Sci* **2**: 174-183, 1998.
- WATSON A, NACHMIAS J: Pattern of temporal integration in localised population in the detection of grating. *Vision Res* **17**: 893-902, 1977.
- ZEEMAN E: Duffing's equation in brain modelling. *Bull Inst Math Appl* **12**: 207-214, 1976a.
- ZEEMAN E: Brain modelling, structural stability, the theory of catastrophes and applications in the sciences. In: *Lecture Notes in Math*. Springer-Verlag Heidelberg, 1976b, pp 367-372.
-

Reprint requests

Dr. J. Kremláček, Medical Faculty, Charles University, Šimkova 870, 500 01 Hradec Králové, Czech Republic, e-mail: jan.kremlacek@lfhk.cuni.cz

Fig. 3. Recorded (thin solid line) and simulated (bold solid line) motion-onset VEPs to slowly moving (7 deg/s) high contrast (96 %) checkerboard (0.75 deg^{-1}). The contributions of separate oscillators are drawn as dotted (OSC1), broken (OSC2) and broken-dotted (OSC3) line. The NRMSE between recorded and simulated data is 11.85 %.

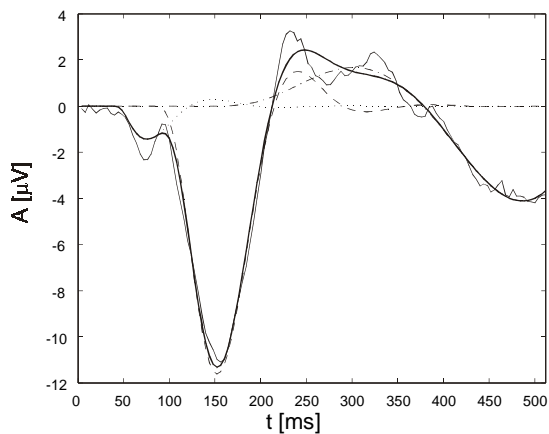


Fig. 4. Recorded and simulated motion-onset VEPs to fast moving (14 deg/s) low contrast (10 %) structure of isolated checks (0.375 deg^{-1}). The figure arrangement is the same as in Fig. 3. The NRMSE between recorded and simulated data is 12.90 %.

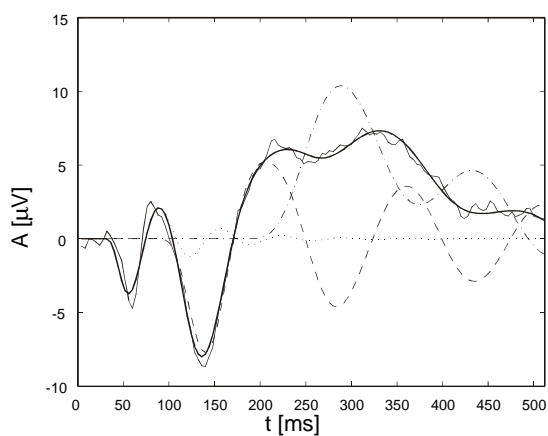


Fig. 5. Recorded and simulated P-VEPs to the pattern-reversal of high contrast (96 %) checkerboard (0.75 deg^{-1}). The figure arrangement is the same as in Fig. 3. The NRMSE between recorded and simulated data is 10.97 %.

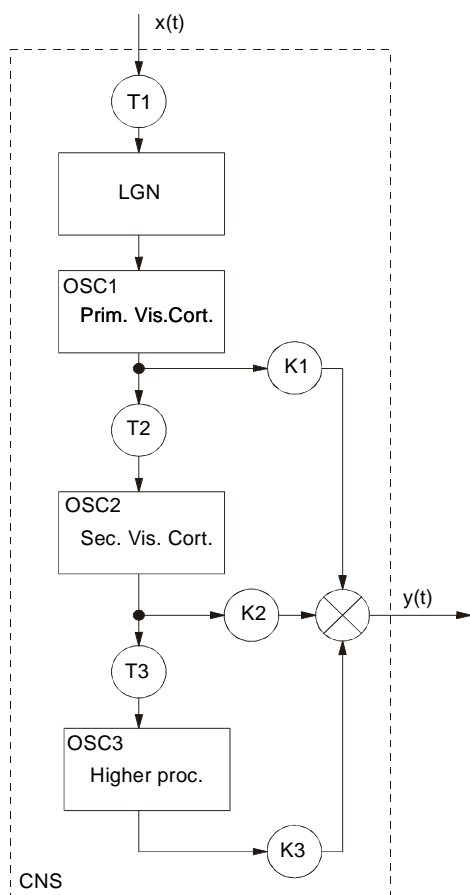


Fig. 1. Block diagram of visual evoked potentials generation. The model is forced with delay T_1 from LGN. Following oscillators represent cortical neural groups activated with a delay T_n and contributing to the final potential according to the weight coefficients K_n . The OSC_1 epitomises the primary visual cortex, the OSC_2 extrastriate areas and a response of OSC_3 mimics probably a higher level of perception.

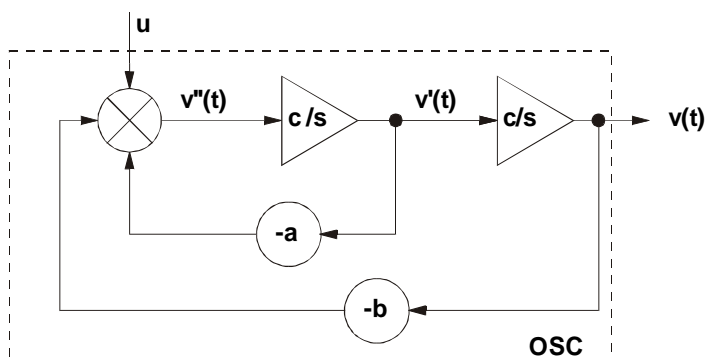


Fig. 2. The schema of the single oscillator as it was modeled in Simulink. The oscillator can be described by the following nonlinear second order equation: $\ddot{v} = u(t) - av - bv$.